J Mol Model (2014) 20:2473
DOI 10.1007/s00894-014-2473-4

ORIGINAL PAPER

The role of NH_3 and hydrocarbon mixtures in GaN pseudo-halide CVD: a quantum chemical study

Oleg B. Gadzhiev · Peter G. Sennikov · Alexander I. Petrov · Krzysztof Kachel · Sebastian Golka · Daniela Gogova · Dietmar Siche

Received: 7 May 2014 / Accepted: 21 September 2014 / Published online: 15 October 2014

Abstract The prospects of a control for a novel gallium nitride pseudo-halide vapor phase epitaxy (PHVPE) with HCN were thoroughly analyzed for hydrocarbons–NH_3–Ga gas phase on the basis of quantum chemical investigation with DFT (B3LYP, B3LYP with D3 empirical correction on dispersion interaction) and ab-initio (CASSCF, coupled clusters, and multireference configuration interaction including MRCI+Q) methods. The computational screening of reactions for different hydrocarbons (CH_4, C_2H_6, C_3H_8, C_2H_4, and C_2H_2) as readily available carbon precursors for HCN formation, potential chemical transport agents, and for controlled carbon doping of deposited GaN was carried out with the B3LYP method in conjunction with basis sets up to aug-cc-pVTZ. The gas phase intermediates for the reactions in the Ga-hydrocarbon systems were predicted at different theory levels. The located π-complexes Ga…C_2H_2 and Ga…C_2H_4 were studied to determine a probable catalytic activity in reactions with NH_3. A limited influence of the carbon-containing atmosphere was exhibited for the carbon doping of GaN crystal in the conventional GaN chemical vapor deposition (CVD) process with hydrocarbons injected in the gas phase. Our results provide a basis for experimental studies of GaN crystal growth with C_2H_4 and C_2H_2 as auxiliary carbon reagents for the Ga-NH_3 and Ga-C-NH_3 CVD systems and prerequisites for reactor design to enhance and control the PHVPE process through the HCN synthesis.

Keywords Computer simulation · Density functional theory · Gallium compounds · Growth models · Semiconducting III-V materials · Vapor phase epitaxy

Introduction

Gallium nitride (GaN) is a semiconductor, characterized by a unique combination of properties (wide direct band-gap, higher thermal conductivity, large free exciton and optical phonon energies) which makes it highly advantageous for high-frequency and high-power electronic devices, blue–ultraviolet light-emitting diodes (LEDs), and laser diodes. However, no really cost efficient growth technique is available for the fabrication of bulk GaN crystals, from which substrate wafers could be prepared.

Hydrogen cyanide (HCN) is a chemical transport agent in a novel Ga-C-NH_3 or so called pseudo-halide vapor phase epitaxy (PHVPE) chemical transport system [1–3] as it has already been demonstrated on the basis of thermodynamic consideration [2] and quantum chemical mechanistic study [4]. However, for the PHVPE method [1–3] based on heterogeneous reaction between solid graphite and NH_3 to release in the reactor volume the chemical transport reagent (HCN) one can reveal a potential shortcoming to develop an effective and scalable CVD GaN method: it is mostly uncontrolled

Electronic supplementary material The online version of this article (doi:10.1007/s00894-014-2473-4) contains supplementary material, which is available to authorized users.

O. B. Gadzhiev · P. G. Sennikov
G.G. Devyatykh Institute of Chemistry of High-Purity Substances, Russian Academy of Sciences, 49 Troponina St., Nizhny Novgorod 603950, Russia

O. B. Gadzhiev (✉)
N.I. Lobachevsky State University of Nizhny Novgorod, National Research University, 23 Gagarin Avenue, Nizhny Novgorod 603950, Russia
e-mail: euriscomail@mail.ru

A. I. Petrov
Sibirian Federal University, 81 Svobodny prosp., Krasnoyarsk 660041, Russia

K. Kachel · S. Golka · D. Gogova · D. Siche
Leibniz Institute for Crystal Growth, Max-Born-Str. 2, 12489 Berlin, Germany

generation of the carbonic atmosphere due to inherent features of the exploited heterogeneous reactive system. Hence, to bypass the technological problem, we need to investigate the gas phase reactions of HCN generation since it is expected to control the process by means of an injection system. First of all, we consider the reactivity of CH_4 with NH_3 and Ga vapor because one can anticipate that the reaction $CH_4+NH_3 \rightarrow HCN+3H_2$ can be an important and abundant source of the chemical transport reagent. We suppose that reactions of C_2H_6 and C_3H_8 (homologues of CH_4) or C_2H_4 and C_2H_2 with NH_3 or Ga(^{2}P) can be sources of reactive intermediates if the corresponding reactions are not hindered.

Reactivity of Ga atoms was studied previously experimentally and theoretically by using quantum chemical methods (see reviews [5, 6] and references therein) for different electronic states and therefore, for different approaches to stimulate the reaction (thermal or photo-activation). For the present study, it is important to note that the direct insertion reaction $Ga+CH_4 \rightarrow CH_3GaH$ was investigated earlier by the matrix isolation technique with the matrix UV–irradiation combined with electron spin resonance (ESR) spectroscopy, ab–initio quantum chemical calculations [7, 8] as well as IR–spectroscopy method and DFT calculations [9]. It was found that CH_4, Ga, CH_3GaH, CH_3Ga, Ga_2, and non assigned Ga_n clusters were entrapped in the rigid matrix [9].

In ref. [10] profiles of several potential energy surfaces (PESs) for the $Ga+CH_4$ system were constructed by a special procedure with energy calculations by multi–reference configuration interaction with perturbation selection through iterations (CIPSI) method [11, 12] which provides energy as the sum of the variational energy in the reference space and a second-order Möller-Plesset (MP2) energy contribution from the determinants outside the reference space. The reference CAS(11,12)SCF wave function was expanded on relativistic effective core potential (RECP) with triple-ζ spd–valence basis set augmented by s–, p–, and d–diffuse basis functions [10] for Ga and RECP with double-ζ sp-valence basis set extended by polarization d-function for C, and 1 s double-ζ basis set extended by p–polarization function for H atoms. It was shown that Ga(^{2}S) reacts with CH_4 via conical intersection of the ground and the excited state PESs whereas barrier height for Ga(^{2}P) was estimated to be 53.7 kcal mol^{-1} [10]. Transition probabilities between electronic states reported in ref. [10] were estimated in ref. [13].

The Ga(^{2}P)+C_2H_2 and Ga(^{2}P)+C_2H_4 reactions with varied concentrations of hydrocarbons were studied [7, 14, 15] by a combination of Ar matrix isolation technique and low level quantum chemical calculations with MP2(FC)/3-21G(2d) as the highest one. In refs. [7, 14, 15], the quantum chemical methods were employed to search intermediates and to interpret experimental ESR and IR spectral data. Structures of π–complexes Ga…C_2H_2…Ga, Ga…C_2H_2, Ga…C_2H_4, Ga…$(C_2H_4)_2$ were reported in [7, 14, 15]. However, no reaction mechanisms were established earlier. Therefore, it is of great interest to study the reactivity of simple gas phase hydrocarbons, namely, CH_4, C_2H_6, C_3H_8, C_2H_2, and C_2H_4, in the thermally activated reaction with Ga(^{2}P).

The CH_4 (and its homologues), C_2H_2 and C_2H_4 are representatives of different classes of hydrocarbons. Thus, in the chosen set, the assessment of their reactivity trend with carbon chain increase is an important feature of computational screening. For the Ga–hydrocarbon–NH_3 system, one can assume a catalytic activity or reactivity of Ga…hydrocarbon complex on the $Ga+NH_3$ insertion reaction or on reactions in the NH_3+hydrocarbon system. These reactions will be studied with quantum chemical methods.

The goal of the presented study is to predict gas phase reaction mechanisms for the Ga–hydrocarbon (CH_4, C_2H_6, C_3H_8, C_2H_4, and C_2H_2) –NH_3 systems in the ground state on a basis of quantum chemical investigation. As a result, the prospects of control for PHVPE through HCN synthesis in the hydrocarbon–NH_3 reaction will be estimated. Additionally, we will elucidate the physico-chemical background of carbon incorporation in the case of injection of the carbon precursor in the gas phase. It is indispensable to reveal key–intermediate(s) in the gas phase since they are carried by dilute gas flow on the surface layer and, thus, can cause the carbon doping of growing GaN crystal and after passing the reactor's exhaust can be trapped and detected in further experimental investigation.

The computational screening of different hydrocarbons (CH_4, C_2H_6, C_3H_8, C_2H_4, and C_2H_2) as potential chemical transport agents and for controlled carbon doping of deposited GaN assists in the interpretation of the experimental results and excludes an influence of the particular choice of chemical reactor design or/and operational conditions.

Computational details

For preliminary stationary point search in the Ga–C_xH_y–NH_3 systems and the PES topography exploration the B3LYP/cc-pVDZ (C,H)+cc-pV(D+d)Z (Ga) theory level was employed. These calculations were carried out with GAMESS program [16]. The reactants, intermediates, and transition states (TSs) were optimized further at the B3LYP/cc–pVTZ [17–22] theory level by means of GDIIS method [23] as implemented in the Gaussian 03 suite of programs [24]. ChemCraft [25] and GaussView3 [26] molecular builders and editors were used as tools for visualization and further analysis of the results obtained. This theory level was chosen consistent with an earlier study [4] of reaction mechanisms for the gas-phase model of the pseudohalide CVD in the NH_3-graphit-Ga system. In the present study, the located structures were re-optimized with the augmented basis set at the B3LYP/aug-cc-pVTZ theory level to reduce basis set superposition error (BSSE) which can

be especially important for atomic–molecular complexes and other floppy structures including TSs.

Harmonic vibration frequency calculations with analytic Hessian evaluation were conducted for all the stationary points to insure their correct assignment to local minima (all vibrational frequencies are positive) or transition states (single imaginary frequency). Minimum energy paths (MEPs) were constructed between all found stationary points by means of intrinsic reaction coordinate (IRC) calculations [27, 28].

This hybrid GGA functional includes three parameters determined by fitting on the G1 data set [29]. Numerous assessments and benchmarks of DFT methods found that results of calculations by B3LYP functional were comparable or even better than results of other functionals [30]. The B3LYP density functional became quite popular and is widely applied to chemical problems including GaN MOCVD in Me_3Ga+NH_3 [31–33] and other metal organic sources of Ga [34, 35]. However, the performance of available density functionals for prediction of structural parameters, reaction and activation energies is limited [36–38] if middle-range electron correlation effect is required to be covered or even the PES topologies as determined with different quantum chemical methods are qualitative different [39–42].

In addition, taking this into account, the atomic-molecular complexes were optimized at the B3LYP/aug-cc-pVTZ+D3 theory level where D3 denotes an empirical dispersion correction [36–38]. Located π-complexes were optimized at the CCSD/aug-cc-pVTZ theory level with subsequent energy refinement with the composite approach CCSD(T)/aug-cc-pVTZ//CCSD/aug-cc-pVTZ.

The PES profile obtained with the B3LYP method for the $CH_4+Ga(^2P)\rightarrow TS\rightarrow HGaCH_3$ reaction was verified at the CAS(11,12)SCF/cc-pVDZ theory level. Next, the activation energy was estimated by means of IRC curve following approach [43–47], that is, dual−level approximation for the quantitative estimation of the activation energy (E_a) without full optimization of the geometric parameters in the vicinity of two stationary points (different formalisms are reviewed in [48, 49]). Here, E_a was calculated with the MRCI+Q method in conjunction cc-pVTZ and aug-cc-pVTZ basis sets on the structures of the IRC curves obtained at the B3LYP/cc-pVTZ and B3LYP/aug-cc-pVTZ theory levels, respectively. The augmentation of the cc-pVTZ basis set was used for estimation of influence of diffuse function and to provide computational results in quantitative consistency with the theory level of ref. [10]. To justify the results obtained with the MRCI+Q method, a set of the IRC curve following calculations at the MR-DDCI-1/cc-pVTZ and MR-DDCI-3/cc-pVTZ theory levels was completed. The ORCA suite of programs [50, 51] was employed for the calculations with the MRCI+Q, MR-DDCI-1, MR-DDCI-3, and B3LYP+D3 methods.

Results and discussion

Reactivity of CH_4, C_2H_6, C_3H_8, C_2H_4, and C_2H_2 in reactions with NH_3

The chemistry of both reagents (CH_4 or other alkanes and NH_3) is well–known and is a fundament of important technological processes [52]:

1) In the Blausäure–Methan–Ammoniak (BMA, or HCN–methane-ammonia) process developed by Degussa around 1949 in cooperation with Heinrich Koppers GmbH HCN is synthesized from methane and ammonia:

$$NH_3 + CH_4 \rightarrow HCN + 3H_2 (\Delta_r H = +256\,kJ/mol, 1300^\circ C, catalysis-Pt/Ru) \quad (1)$$

2) Shawinigan Chemicals (Canada) developed the Fluohmic process around 1960. In the Shawinigan process (Shine, 1971) hydrocarbon gases (usually propane or butane) are reacted with ammonia in a fluidized bed consisting of coal particles, which are directly heated with electric current:

$$3NH_3 + C_3H_8 \rightarrow 3HCN + 7H_2 (\Delta_r H = +605\ kJ/mol\ HCN,\ 1350-1650^\circ C). \quad (2)$$

The conditions required for both processes (high temperature and/or catalysts) are not realized for the typical PHVPE GaN crystal growth.

Let us investigate gas phase reactions (3)–(7) of HCN synthesis, (9), (10) substitution for C_2H_6 and C_3H_8, and the direct addition reactions (11), (12) at the B3LYP/cc-pVTZ theory level:

$$CH_4 + NH_3 \rightarrow CH_3NH_2 + H_2 \quad (3)$$

$$CH_3NH_2 \rightarrow HCNH_2 + H_2 \quad (4)$$

$$CH_3NH_2 \rightarrow H_2CNH + H_2 \quad (5)$$

$$HCNH_2 \rightarrow HCN + H_2 \quad (6)$$

$$H_2CNH \rightarrow HNC + H_2 \quad (7)$$

$$H_2CNH \rightarrow HCNH_2 \quad (8)$$

$$C_2H_6 + NH_3 \rightarrow CH_3CH_2NH_2 + H_2 \quad (9)$$

$$C_3H_8 + NH_3 \rightarrow (CH_3)_2CHNH_2 + H_2 \quad (10)$$

$$C_2H_4 + NH_3 \rightarrow CH_3CH_2NH_2 \quad (11)$$

$$C_2H_2 + NH_3 \rightarrow CH_2CHNH_2. \quad (12)$$

Structures and corresponding Cartesian coordinates for the transition states of the reactions (3)–(7), (9)–(12) were collected in Supporting information (Fig. 1S and Table 1S).

The activation energy for elementary substitution (3) reaction is 494.5 kJ mol^{-1} as calculated at the B3LYP/cc-pVTZ level of theory. Amine CH_3NH_2 can undergo dehydrogenation reactions (4) and (5) with formation of carbene $HCNH_2$ and imine H_2CNH. The E_a values for the reactions (4) and (5) are 340.6 and 490.5 kJ mol^{-1}, respectively. The HCN formation in the reaction (6) through dehydrogenation of carbene is undergone with the barrier height of about 298.5 kJ mol^{-1}. The reaction path (7) with HNC formation is highly activated with the barrier height of 375.9 kJ mol^{-1}. For the isomerization $H_2CNH \rightarrow HCNH_2$ (8), the activation energy is 356.0 kJ mol^{-1}. Thus, the calculated data for (3)–(8) is in agreement with experimentally determined very low reactivity of CH_4 with NH_3 and necessity to employ catalysis, e.g., like in Degussa's BMA technological process.

The elementary substitution (9), (10) and addition (11), (12) reactions, which can be considered as initial stages of gas phase HCN synthesis from the hydrocarbons, are very highly activated as determined at the B3LYP/cc-pVTZ theory level. For all the structures of the transition states for H_2 elimination, the quasi-cyclic four-membered CH…HN moiety with elongated C-H and N-H bonds can be clearly assigned (Fig. 1S). The activation energies are given as 480.7, 472.7, 233.1, and 162.9 kJ mol^{-1} for reactions (9), (10), (11), and (12), respectively. The corresponding reaction energies are given as the following: 99.4, 90.5, −61.2, and −134.0 kJ mol^{-1}. The barrier heights for C_2H_6 and C_3H_8 (reactions 9 and 10) are insignificantly lower than the one for CH_4. Thus, the hydrocarbons (CH_4, C_2H_6, and C_3H_8) do not provide reaction pathway to HCN in the gas phase of GaN PHVPE.

To our knowledge, the reactions (11) and (12) are not included in any technological process. To be realized for HCN synthesis, the highly activated stage of C-C bond cleavage (with activation energy of about 380 kJ mol^{-1}) is required to be overcome for the reactions (11) and (12), and is considered here for completeness of the computational screening.

Reactivity of Ga with CH_4, C_2H_6, and C_3H_8

In the presented study, we investigate the elementary C–H–bond insertion reaction for Ga(^{2}P) and CH_4, C_2H_6, and C_3H_8 (for propane, both primary and secondary carbon atoms were considered as reactive centers). It is worth noting that the reaction and activation energies calculated at the B3LYP/cc-pVTZ and B3LYP/aug-cc-pVTZ theory levels are in very good agreement (within a few kJ mol^{-1}). An exclusion, i.e., in the NH_3 association reaction with Ga…C_2H_2 and Ga…C_2H_4, the binding energy is basis set dependent. Thus, to be consistent with the data reported in ref. [4] and provide easy comparison of reaction pathways, the values are reported for the B3LYP/cc-pVTZ theory level. Corresponding values obtained with aug-cc-pVTZ basis set are assembled in Tables 1 and 3. The optimized Cartesian coordinates are given in Supporting information (Tables 1S and 2S for the calculations at the B3LYP/cc-pVTZ and B3LYP/aug-cc-pVTZ theory levels). The structures of all the found TSs (**TS1**–**TS4**) include the quasi–cyclic three membered C…H…Ga fragment (Fig. 1, Table 1S).

For the Ga+C_2H_6 (system B in Fig. 2), two alternative reaction pathways with **TS2** and **TS3**, respectively, were identified. The saddle points **TS2** (symmetry point group C_1) and **TS3** (symmetry point group C_s) were located for the staggered conformation of ethane; however, they differ in the direction of Ga atom attack (Figs. 1 and 2) and, thus, the values of dihedral angles defined by C-C…H…Ga atoms — about 0° and 90° for **TS2** and **TS3**, respectively, as calculated with the B3LYP method. For **TS2** its symmetry analog exists, **TS2*a***, determined by an approach of Ga atom from symmetry plane; however, it is a structural equivalent. The structures **2** and **3** (symmetry point groups C_1) were located by means of the IRC calculations as product valleys for **TS2** and **TS2*a***, respectively. However, for the symmetric **TS3** and the corresponding reaction path, the structure following downhill to **3** necessarily breaks the symmetry ($C_s \rightarrow C_1$). Therefore, a bifurcation point exists on the reaction path [53, 54]. This conclusion was verified by IRC calculations in the internal coordinates. In this case, the downhill path finished in the TS of degenerate rearrangement between **2** and **3**. In other words, **2**

Table 1 Activation (E_a, kJ mol^{-1}) and reaction (E_r, kJ mol^{-1}) energies for reactions of Ga with CH_4, C_2H_6, C_3H_8, C_2H_2, and C_2H_4 as calculated at the B3LYP/cc-pVTZ and B3LYP/aug-cc-pVTZ theory levels

Reaction	E_a, kJ mol^{-1}[a]	E_r, kJ mol^{-1}[a]
Ga+CH_4→TS1 → → VRI point→1	195.4 (193.9)	37.0 (34.6)
Ga+C_2H_6→TS2→2	161.2 (160.0)	43.5 (41.6)
Ga+C_2H_6→TS2*a*→3		
Ga+C_2H_6→TS3 → → VRI point→2 or 3	160.2 (158.7)	43.5 (41.6)
Ga+C_3H_8→TS4 → → VRI point→4	155.7 (154.0)	49.5 (47.1)
Ga+C_2H_2		
Ga+C_2H_2→TS5→5	22.3 (23.1)	−46.8 (−47.5)
5→TS6→6	3.1 (3.3)	−9.6 (−11.8)
Ga+C_2H_4		
Ga+C_2H_4→TS7→7	25.1 (23.1)	−44.3 (−44.7)
7→TS8→8	304.8 (302.4)	300.7 (295.7)

[a] Data for B3LYP/aug-cc-pVTZ are given in parenthesis

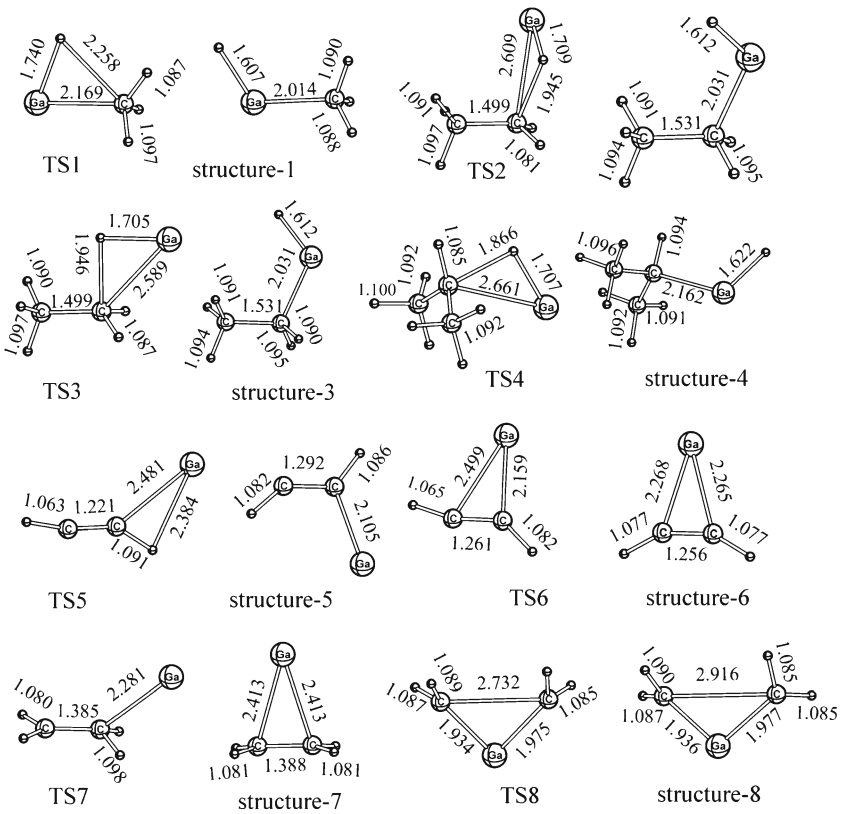

Fig. 1 Structures corresponding to transition states and local minima of PESs optimized at the B3LYP/cc-pVTZ theory level. Bond lengths are given in Å

and **3** are structural analogues with E_a of the conformational isomerization of 0.08 kJ mol^{-1} (Fig. 3); however, their existence is of especial importance for determination of topology of the PES fragment and, thus, is important not only for local rather than for global features of the PES. Bifurcation point for this case coincides with valley-ridge inflection point that was determined in ref. [4] for the Ga-NH_3 insertion reaction as well as in ref. [39] associated with degenerate rearrangement.

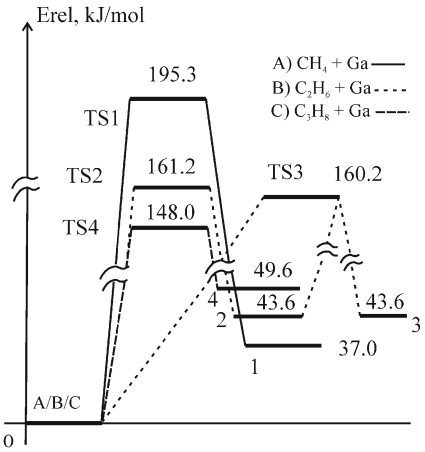

Fig. 2 The PES profiles corresponding to reactions of Ga with CH_4, C_2H_6, and C_3H_8 system were obtained at the B3LYP/cc-pVTZ theory level. The relative energies are in kJ mol^{-1}. The solid, dotted and dashed lines depict reaction pathways for CH_4+Ga(^{2}P), C_2H_6+Ga(^{2}P), and C_3H_8+Ga(^{2}P), respectively

Similarly, bifurcation points on reaction paths were detected for the Ga-CH_4 and Ga-C_3H_8 systems after **TS1** and **TS4**, respectively. Both transition states belong to C_s symmetry point group. Structures corresponding to saddle points of the conformational rearrangements with E_a of 0.3 and 7.2 kJ mol^{-1} for Ga-CH_4 and Ga-C_3H_8, respectively, are depicted in Fig. 3. Both TSs belong to the symmetry breaking paths where the symmetry point groups of structures change from C_s to C_1. Defined in the early 1980s in [55–58], bifurcation point on PESs is a challenge for ongoing developments of mathematical grounds and computational algorithms [59–63] and physico-chemical applications [59, 64–70].

The stabilization energy for all located pre–reactive complexes are estimated to be very small (not more than 0.01 kJ

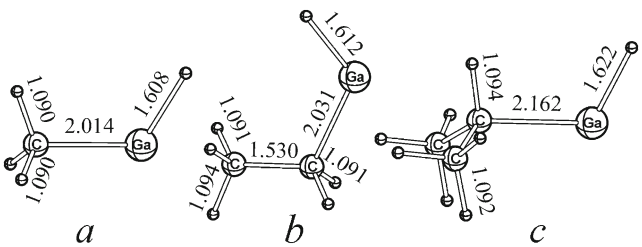

Fig. 3 On the detection of the valley–ridge inflection points on minimum energy reaction path. Transition state structures for degenerate rearrangements located at the B3LYP/cc-pVTZ theory level: (**a**) $CH_3GaH \rightarrow CH_3GaH$; (**b**) $CH_3CH_2GaH \rightarrow CH_3CH_2GaH$, and (**c**) $(CH_3)_2CHGaH \rightarrow (CH_3)_2CHGaH$

mol^{-1}) at the B3LYP/cc-pVTZ theory level, and their structures are very loose with typical shortest Ga…H distance of about 3.1 Å (Supporting information, Table 1S). The complex stabilization energy and the Ga…H distance calculated with B3LYP+D3 method were found to be 7.5 kJ mol^{-1} and 3.05 Å, respectively, for CH_4 as a representative of alkanes. The activation energies of the reactions are 195.4 kJ mol^{-1} for **TS1**, 161.2 kJ mol^{-1} for **TS2**, 160.2 kJ mol^{-1} for **TS3**, and 155.7 kJ mol^{-1} for **TS4** (systems A, B, and C, respectively, in Fig. 2). For Ga atom approach to primary H atom of C_3H_8 similar to **TS2** of the Ga-C_2H_6 system, E_a was found to be 162.1 kJ mol^{-1}. As is known, the primary H atoms are less reactive than secondary H atoms in hydrocarbons. The computational results are in agreement with this experimental trend as can be deduced from the reaction energies comparison. The corresponding reactions are moderately endothermic, i.e., the relative energies of **1**–**4** are 37.0, 43.5, 64.2, and 49.5 kJ mol^{-1}, respectively. The activation (E_a) and reaction (E_r) energies for the reactions in the Ga-hydrocarbon systems are presented in Table 1.

In earlier studies [5, 6, 10], the analysis of probable influence of non–dynamic electron correlation for the **TS1** was not presented. Here, we performed the analysis of the wave function obtained with full geometry optimization at the CAS(11,12)/cc-pVDZ theory level. One can note that the structure of **TS1** located with CASSCF method is similar to the optimized one in DFT calculations (Table 1S). The inspection of the configuration interaction (CI) amplitudes for CAS(11,12)/cc-pVDZ wave function shows that the relative weight of the Hartree-Fock configuration (the square of the first coefficient in the CI expansion vector) is about 0.93. Thus, it is likely that results of the B3LYP density functional as a single reference method are reliable. The E_a value was calculated with the MRCI+Q/cc-pVTZ//B3LYP/cc-pVTZ (Table 3S) and MRCI+Q/aug-cc-pVTZ//B3LYP/aug-cc-pVTZ (Table 4S) composite approaches with the IRC curve following approximation to validate the correctness of treatment of dynamic correlation effect on the PES profile of CH_4+Ga→**TS1**→$HGaCH_3$ by the B3LYP method. The E_a values refined with the MRCI+Q method and calculated at the B3LYP/cc-pVTZ theory level are 208.5 (with the cc-pVTZ basis set), 204.4 (with the aug-cc-pVTZ basis set), and 173.3 kJ mol^{-1}, respectively. The difference between the MRCI and B3LYP results in one basis set is 13 kJ mol^{-1} that is less than the mean absolute deviation (MAD) for this density functional (determined in [30] to be 17.3 kJ mol^{-1}) and is 6.2 % of E_a estimated at the MRCI+Q/cc-pVTZ level and, thus, one can consider it to be in good agreement. The basis set augmentation has a very moderate effect, i.e., the difference is 4.1 kJ mol^{-1}, thus, it is comparable with the chemical accuracy threshold. No intruder states problem was detected for the multi-reference calculations on the supermolecular (Ga…CH_4) system for the reactant valley and the saddle point (Figs. 2S and 3S). Therefore, taking into account close agreement between values of activation energy calculated at the B3LYP/cc-pVTZ theory level and with the MRCI+Q method in conjunction with the IRC curve following approximation and the observed coincidence of the PESs topologies determined by stationary point search and IRC calculations with the B3LYP and CASSCF methods, one can conclude that DFT-B3LYP density functional is reliable for the activation energy estimation of the Ga insertion reaction and investigation of the PES topology for the PES fragment corresponding to the reaction. The E_a of 224.6 kJ mol^{-1} calculated earlier in [10] with the wave function of the CIPSI method expanded on triple-ζ, spd–valence basis set augmented by s–, p–, and d–diffuse basis functions for Ga and RECP with double-ζ, sp-valence basis set extended by polarization d-function for C, and 1s double-ζ basis set extended by p–polarization function for H atoms sets with diffuse functions for C and H atoms is about 20.2 kJ mol^{-1} (10 %) higher than the estimate at the MRCI+Q/aug-cc-pVTZ theory level. This discrepancy was analyzed further, first, on limitation of MR-CISD+Q wave function by means of MR-DDCI-3 and MR-DDCI-1 calculations updating the IRC curve obtained at the B3LYP/cc-pVTZ theory level (the multireference methods are ordered here from the most flexible to least flexible wave function), second, on basis set extension for all electron basis set, and, third, on implicit coverage of relativistic effect by effective core potential.

The estimated E_a values for the multireference DDCI-3 and DDCI-1 methods are 209.0 and 194.7 kJ mol^{-1} and, thus, two conclusions can be deduced: 1) MR-DDCI-3 wave function is a very good approximation to MR-CISD+Q; 2) truncation of the wave function does not provide value higher than one calculated with the MRCI+Q method. CIPSI is a hybrid method providing the total energy as the sum of the variational energy in the reference space and a second-order Möller-Plesset (MP2) energy contribution from the determinants outside the reference space. Thus, the energy terms can be overestimated if the quasi-degenerate orbitals are involved in the space. One can conclude that MRCI+Q method implemented in ORCA being a more elaborated version of CASSCF-based methods provides a more reliable result.

The basis set extension from aug-cc-pVTZ to aug-cc-pVQZ for CCSD(T) provides a very small influence on E_a given as 158.1 and 160.1 kJ mol^{-1}, respectively. If for Ga the aug-cc-pVTZ-PP pseudo-potential basis set with inner ten electrons approximated by the effective core potential was used, the activation energy calculated with the CCSD(T)/aug-cc-pVTZ-PP(Ga)+aug-cc-pVTZ(C,H)//B3LYP/aug-cc-pVTZ composite approach is 149.6 kJ mol^{-1}. Hence, the employed here aug-cc-pVTZ basis set is reliable for energy calculations.

The trend determined here of reactivity from less reactive to more reactive in the sequence of CH_4 – C_2H_6 – C_3H_8 (for the latter, the insertion reactions for the C–H bond of the

primary and secondary carbon atom are considered here) is very common for chemistry of hydrocarbons. Moreover, comparison of activation energies for $Ga(^2P)+NH_3 \rightarrow HGaNH_2$ calculated in refs. [4, 71] results in significantly less reactivity than for NH_3 which in turn is less reactive than HCN [2, 4]. Thus, the reactions of CH_4 and its homologues with $Ga(^2P)$ in thermal activated conditions are highly unfavorable and hindered. Hence, these hydrocarbons (CH_4, C_2H_6, and C_3H_8) are not the favored candidates for an efficient chemical transport with carbon doping based on HCN formation or in the form of reactive carbon intermediates.

Reactivity of $Ga(^2P)$ with C_2H_2 and C_2H_4

The calculations performed in the presented study reveal that the T–shaped π–complex Ga…C_2H_2 (**6**) is formed in a step–wise reaction which proceeds via **TS5**, intermediate **5** and **TS6** with activation energies (E_a) of the first and second step of 22.3 and about 3.1 kJ mol^{-1} (Figs. 1 and 4, Table 1). The relative energy of the complex **5** is −46.8 kJ mol^{-1}. The energy of the association reaction calculated with B3LYP+D3 method is −58.5 kJ mol^{-1}. To our knowledge, the structure **5** with trans–oriented H atoms was not reported earlier for Ga/C_2H_2 complexes. However, a complex with similar structure was reported [72] for Al. In contrast to **6** with two equivalent Ga…C atomic molecular bond lengths of about 2.268 Å, **5** is characterized by two non equivalent bond lengths — 2.108 Å and 2.568 Å (Fig. 1 and Table 1S); **6** is thermodynamically more favorable than **5** by about 8.5 (8.4) kJ mol^{-1}. The value calculated with D3 correction is given in parenthesis.

The reaction $Ga+C_2H_4 \rightarrow$ **7** was found to proceed through a single saddle point **TS7** with E_a=25.1 kJ mol^{-1} and reaction energy −44.3 (−57.8) kJ mol^{-1} (Fig. 4). The skewed approach

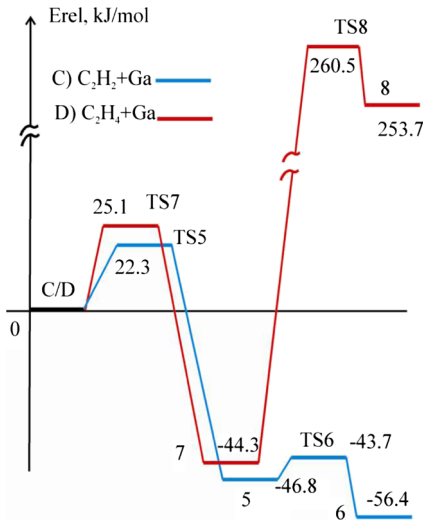

Fig. 4 The PES profiles corresponding to reactions of Ga with C_2H_2 (system C) and C_2H_4 (system D) were obtained at the B3LYP/cc-pVTZ theory level. The relative energies are given in kJ mol^{-1}

through **TS7** is an elementary reaction in contrast to the π–complex (**6**) formation for acetylene. No pre-reactive complex was located for this reaction. The structure corresponding to a reagent valley from IRC calculations rearranged after full geometry optimization to a very shallow T-shaped complex with elongated up to 3.2 Å Ga…C bond lengths (Table 1S). The double-well potential, i.e., two T-shaped complexes, was assigned in the earlier study [7] to $^2B_2$ and $^2B_1$ electronic states for "tight" and "loose" structures, respectively.

Taking into account limited performance of available DFT methods for systems stabilized by medium range electron correlation and the determined earlier in [4] difference within a few dozen kJ mol^{-1} between the B3LYP and CCSD(T) data, especially, for Ga-Ga compounds, the π-complexes **6** and **7** were optimized with symmetry restriction, that it, point group C_{2v} as was determined in the full geometry optimizations with the B3LYP method, at the CCSD/aug-cc-pVTZ theory level and the association reaction energies were refined at the CCSD(T)/aug-cc-pVTZ theory level. The Ga…C bond lengths are 2.198 and 2.293 Å in **6** and **7**, respectively. The calculated values are by about 0.07 and 0.12 Å less than those optimized with the B3LYP method. Corresponding reaction energies at the CCSD(T)/aug-cc-pVTZ theory level are estimated to be −74.9 and −67.5 kJ mol^{-1} while at the CCSD/aug-cc-pVTZ level used for the geometry optimizations the energies are −63.9 and −57.1 kJ mol^{-1}, respectively.

Taking into account the determined remarkable difference between results obtained with the B3LYP, B3LYP+D3, and CCSD(T) methods, namely, the order of decrease of the reaction energies given as following E_r(B3LYP/cc-pVTZ)> E_r(B3LYP+D3/cc-pVTZ)>E_r(CCSD(T)/aug-cc-pVTZ), i.e., from lower to higher exothermicity, is analyzed further with the basis set augmentation (Table 2) and T_1-diagnostic calculation [73, 74].

The values calculated with the DFT+D3 method are in excellent agreement with those obtained at the CCSD/aug-cc-pVTZ theory level (Table 2) for both basis sets. However, the coupled cluster method exhibited remarkable differences in the provided results: −51.9 and −63.9 kJ mol^{-1} for **6** and −40.9 and −57.1 kJ mol^{-1} for **7** with cc-pVTZ and aug-cc-pVTZ

Table 2 Reaction energy (E_r, kJ mol^{-1}) for the association of Ga atom with C_2H_2 or C_2H_4 calculated with the B3LYP+D3, CCSD, and CCSD(T) methods

Method/basis set	Reaction energy (E_r, kJ mol^{-1})	
	Ga…C_2H_2 (6)	Ga…C_2H_4 (7)
B3LYP/cc-pVTZ+D3	−66.0	−57.7
B3LYP/aug-cc-pVTZ+D3	−65.6	−57.8
CCSD/cc-pVTZ	−51.1	−40.9
CCSD/aug-cc-pVTZ	−63.9	−57.1
CCSD(T)/aug-cc-pVTZ	−74.9	−67.5

basis sets, respectively. The reported, in the presented study, relative slow convergence of the CCSD calculated energies with basis set augmentation with respect to this one for B3LYP method is well known. T_1 diagnostic values for Ga, C_2H_2, C_2H_4, **6**, and **7** of about 0.012 calculated for coupled cluster method are below the threshold value of 0.02 [73, 74]. Hence, according to the criterion, influence of non-dynamic electron correlation on the CCSD(T) results is insignificant. One can conclude that the results calculated with the CCSD(T)/aug-cc-pVTZ approach are the best estimate. The B3LYP/cc-pVTZ data can be taken as a robust estimate for reaction energies and an extensive screening of reactions, reaction paths, and structures. The B3LYP/cc-pVTZ+D3 competes very efficiently with the significantly more resource and time consuming CCSD/aug-cc-pVTZ theory level. The reaction energies and geometrical parameters reported for the T-shaped complexes **6** and **7** (Fig. 1, Tables 1S and 2S) were optimized in the present study at the computational level better than those reported in refs. [7, 14, 15].

The insertion of Ga atom in the double bond is hindered (E_a=304.8 kJ mol^{-1}) and unlikely to be observed among the thermally activated gas phase reactions. Hence, it is very unlikely that a double carbenoid complex **8** (Fig. 4) and its successor in the reaction path perfectly linear H_2CGaCH_2 (shown in Supporting information) will be formed in an observable amount. For the H_2CGaCH_2 carbenoid, the thermodynamics of the net reaction C_2H_4+Ga→H_2CGaCH_2 (E_r= 142.4 kJ mol^{-1}) reveals that its formation is unfavorable.

The small activation energies (22.3 and 25.1 kJ mol^{-1}) for the **6** and **7** generation allow to propose C_2H_2 and C_2H_4 as prospective candidates for GaN carbon doping in the growth conditions in the Ga-NH_3-C_2H_2 or C_2H_4 systems and as a transport agent for enhancement of the conventional Ga–NH_3 CVD system. In contrast, CH_4, C_2H_6, and C_3H_8 do not significantly affect the carbon incorporation through gas phase reactions in the thermal activation conditions. Thus, HCN generated in C+NH_3 at GaN growth conditions in CVD is the main and the most efficient chemical transport reagent and the source of the carbon doping via heterogeneous reactions of HCN and cyano-and isocyano intermediates (HGaCN, HGaNC, GaCN, and GaNC) located in the previous mechanistic study [4] of the PHVPE system [1–3].

Reactivity of the Ga+NH_3 with CH_4, C_2H_2 or C_2H_4

The π-complexes Ga…C_2H_2 (**6**) (Figs. 1 and 4) and Ga…C_2H_4 (**7**) (Figs. 1 and 4) were located at the B3LYP/(aug)-cc-pVTZ, B3LYP/cc-pVTZ+D3, coupled clusters theory levels. The question arises, whether the π-complexes are able to catalyze the HCN synthesis in the C_2H_2-NH_3 and C_2H_4-NH_3 systems or if there is a change of reaction path, reducing the activation barrier for the Ga…C_2H_2+NH_3 and Ga…C_2H_4+NH_3 addition reactions in comparison to the earlier calculated one [4] for Ga(^{2}P)+NH_3 (see also [71]). One can note that the binding energies of the binary complexes **6**, **7**, and Ga…NH_3 are similar, that is, −56.4, −44.6 kJ mol^{-1} as was determined in the presented study and in ref. [4] –39.4 kJ mol^{-1}. Thus, it is necessary to study the insertion reaction Ga…NH_3+CH_4. Therefore, it is necessary to analyze an opportunity of a catalytic activity which can enhance the probability of the Ga-NH_3→$HGaNH_2$ or Ga-CH_4→$HGaCH_3$ addition reactions. Ternary reactions are relative rare. However, several examples are known [39, 75–77].

No reaction pathways being equivalent to the reactions (11), (12) were determined. The structures corresponding to pre-reactive complexes, saddle points, and products for Ga-NH_3 addition reactions in complexes **9** and **10** are shown in Fig. 5. The PES profiles for the reactions are depicted in Fig. 6. The ternary complexes **9** (Ga…C_2H_2…NH_3) and **10** (Ga…C_2H_4…NH_3) were located at the B3LYP/cc-pVTZ and B3LYP/aug-cc-pVTZ theory levels. The complexation reactions **6**+NH_3→**9** and **7**+NH_3→**10** are moderately exothermic with reaction energies (Table 3) of −24.2 and −32.0 kJ mol^{-1}, respectively. Both **9** and **10** can be formed in step-wise reactions in the ternary systems Ga+C_2H_2 (C_2H_4)+NH_3 when the intermediate formation of the binary complexes Ga…C_2H_2 (C_2H_4) or Ga…NH_3 increases the reaction probability.

The activation energies (E_a) estimated as a difference between the energetic levels of monomers (**6** and NH_3 or **7** and NH_3) and corresponding saddle points (**TS9** or **TS10)** are 143.0 kJ mol^{-1} and 131.5 kJ mol^{-1} as calculated at the B3LYP/cc-pVTZ theory level (Fig. 6). For **9→TS9** and **10→TS10**, E_a values were calculated to be 163.5 and 167.2 kJ mol^{-1}, respectively. The E_a value (94.8 kJ mol^{-1} above initial reagents Ga and NH_3 or 134.2 kJ mol^{-1} if Ga…NH_3 is thermalized) obtained earlier [4] for the Ga(^{2}P)+NH_3→$HGaNH_2$ reaction is remarkably lower (by about 35 kJ mol^{-1}) than the E_a values (143.0 and 131.5 kJ mol^{-1} for non-thermalized prereactive complexes **8** and **9**) for the reactions with π-complexes **6** and **7** (Fig. 6). The inclusion of Ga atom in the π-complexes does not stabilize efficiently either the saddle point **TS9** or **TS10** whereas it stabilizes the

Table 3 Activation (E_a, kJ mol^{-1}) and reaction (E_r, kJ mol^{-1}) energies for reactions of Ga…C_2H_2 (**6**) or Ga…C_2H_4 (**7**) with NH_3 and the reaction Ga…NH_3 with CH_4 calculated at the B3LYP/cc-pVTZ and B3LYP/aug-cc-pVTZ theory levels

Reaction	E_a, kJ mol^{-1}[a]	E_r, kJ mol^{-1}[a]
6+NH_3→9	0 (0)	−24.2 (−17.4)
9→TS9→11	167.2 (163.8)	44.7 (40.3)
7+NH_3→10	0 (0)	−32.0 (−24.9)
10→TS10→12	163.5 (160.6)	2.9 (−2.6)
Ga…NH_3+CH_4→TS11→ →$HGaCH_3$…NH_3	185.6 (185.3)	9.4 (9.3)

[a] Data for B3LYP/aug-cc-pVTZ are given in parenthesis

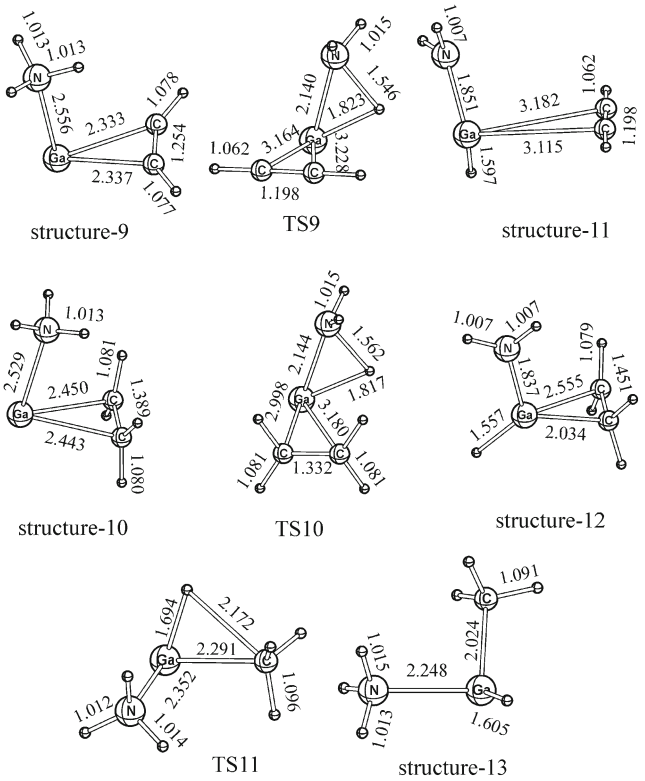

Fig. 5 Structures corresponding to transition states and local minima of PESs optimized at the B3LYP/cc-pVTZ theory level. Bond lengths are given in Å

reactive center. The activation energy Ga…NH_3+CH_4→ **TS11**→CH_3GaH…NH_3 is 185.6 kJ mol^{-1}. The complexation reduced the barrier height by 9.8 kJ mol^{-1} (ca. 5 % of 195.4 kJ mol^{-1} calculated for the Ga+CH_4 system). This difference is less than the MAD value for the B3LYP method [30].

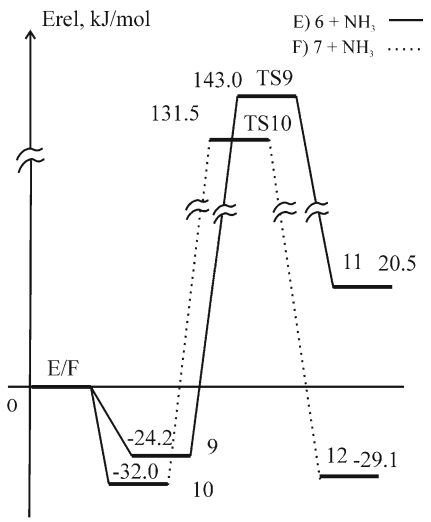

Fig. 6 The PES profiles corresponding to reactions of NH_3 with Ga…C_2H_2 (**6**) and Ga…C_2H_4 (**7**) systems were obtained at the B3LYP/cc-pVTZ theory level. The relative energies are given in kJ mol^{-1}. The solid and dotted lines depict reaction pathways for **6**+NH_3 and **7**+NH_3, respectively

Thus, the rate constant at the temperature T=1000 K through **TS11** is 3.3 times higher than through **TS1**; however, the net reaction including **TS11** is the third-order reaction, that it, the enhancement of the gas phase carbonization reaction can be neglected in comparison with the formation of C_2H_2 and C_2H_4 π-complexes which, thus, are the main gas phase reactive species of GaN crystal carbonization as revealed with DFT and ab-initio methods.

No reduction of the activation barrier was determined at the B3LYP/cc-pVTZ theory level and, thus, no enhancement of GaN CVD with injected hydrocarbons can be proposed with respect to conventional GaN CVD or to the novel PHVPE.

Conclusions

Quantum chemical modeling of gas phase reactions has been carried out to gain insight into controlled chemical transport with HCN as a transport reagent and carbon doping of GaN crystal in carbon-based (Ga-C-NH_3) and conventional carbon-free (Ga-NH_3) CVD systems with injected hydrocarbons. The reactivity of Ga(^{2}P) with hydrocarbons (CH_4, C_2H_6, C_3H_8, C_2H_2, and C_2H_4), which can be considered as easy to use and readily available carbon precursors for both the HCN synthesis and gas phase generation of reactive carbon intermediates, was predicted at the B3LYP/cc-pVTZ theory level. In addition, to exhibit probable catalysis for Ga-NH_3 addition by inclusion of NH_3 and C_2H_4 or C_2H_2 in π-complexes, the potential energy surfaces of the Ga+C_2H_2+NH_3 and Ga+C_2H_4+NH_3 systems were studied.

Using CH_4 as a precursor it is unlikely to obtain HCN in a reaction with NH_3 (only with catalysts) and no reaction with Ga, which results in generation of highly reactive intermediates with low activation energy, was determined at the B3LYP/cc-pVTZ theory level.

C_2H_6 reactivity with Ga(^{2}P) and NH_3 is higher in comparison with CH_4 (activation energies are lower by 35.2 and 13.8 kJ mol^{-1}, respectively); however, HCN cannot be formed efficiently and Ga(^{2}P) cannot act as a catalyst.

C_3H_8 reactant closes the series of the investigated alkanes and is slightly more reactive in comparison in agreement with the common trend for CH_4 homologues.

C_2H_4 low barrier for reacting with Ga(^{2}P) with π-complex C_2H_4…Ga formation but much higher activation energy was estimated to react with NH_3. It is more likely that NH_3 reacts with the product of the Ga+C_2H_4 complexation reaction but inclusion of Ga atom in the complex does not activate the Ga+NH_3→$HGaNH_2$ addition.

C_2H_2 is the most reactive substance between considered hydrocarbons in reactions with both NH_3 and Ga; however, no efficient reaction pathways to HCN or GaN crystal growth precursors were revealed in the present quantum chemical study with the B3LYP density functional.

Taking into account the aforementioned literature data and DFT-B3LYP computational results on the reaction mechanisms and activation energies for elementary stages of reactions between hydrocarbons and ammonia summarized in Table 1, one more conclusion can be drawn regarding process design perspective. To stimulate an HCN synthesis, the PHVPE reactor is required to be equipped by a special block with a properly chosen catalyst. In this case, the control by a gas flow of the reactive $CH_4/NH_3/N_2$ mixture or by concentration of CH_4 can be set up indirectly, that is, by heterogeneous reactions on the catalyst. The novel reactor design with the two-chamber schema (first, for the HCN synthesis, second, for the PHPVE process) can be proposed as an enhancement of the novel PHVPE. A probable catalytic effect of molten Ga surface on the $CH_4+NH_3 \rightarrow HCN+3H_2$ reaction and, thus, *in situ* generation of chemical transport reagent can be a subject of further experimental investigation.

Acknowledgments A.I.P. is thankful to SFU Super-computer Centre (http://cluster.sfu-kras.ru) for generous donation of computer time. O.B.G. is grateful to RFBR and Ministry of Industry and Innovations of Nizhny Novgorod region (Joint Project 13-03-97088). O.B.G. would like to thank Dr. Prof. Stanislav K. Ignatov and Research and Educational Centre "Modern methods of photochemistry, quantum chemistry and spectroscopy" of Chemistry Research Institute, N.I. Lobachevsky State University of Nizhny Novgorod for computer time provided. O.B.G. and D.S. acknowledge fruitful discussions with Dr. Wolfram Miller (Leibniz Institute for Crystal Growth, Berlin, Germany).

References

1. Rost HJ, Siche D, Gogova D, Albrecht M, Jacobs K, Fornari R (2009) The role of carbon in transport processes during PVT growth of bulk GaN. Phys Status Solidi C 6(6):1484–1487. doi:10.1002/pssc.200881523
2. Jacobs K, Siche D, Klimm D, Rost HJ, Gogova D (2010) Pseudohalide vapour growth of thick GaN layers. J Cryst Growth 312(6):750–755. doi:10.1016/j.jcrysgro.2009.12.055
3. Gogova D, Rudko GY, Siche D, Albrecht M, Irmscher K, Rost HJ, Fornari R (2011) A new approach to grow C-doped GaN thick epitaxial layers. Phys Status Solidi C 8(7–8):2120–2122. doi:10.1002/pssc.201001005
4. Gadzhiev OB, Sennikov PG, Petrov AI, Gogova D, Siche D (2013) Gas-phase reactions regarding GaN Crystal growth in a carbon-based transport system: a quantum chemical study. Cryst Growth Des 13(4):1445–1457. doi:10.1021/cg3014738
5. Downs AJ, Himmel H-J, Manceron L (2002) Low valent and would-be multiply bonded derivatives of the group 13 metals Al, Ga and In revealed through matrix isolation. Polyhedron 21(5–6):473–488. doi:10.1016/s0277-5387(01)01036-1
6. Novaro O, Pacheco-Blas MA, Pacheco-Sánchez JH (2012) Potential energy surfaces for reactions of X metal atoms (X=Cu, Zn, Cd, Ga, Al, Au, or Hg) with YH_4 molecules (Y=C, Si, or Ge) and transition probabilities at avoided crossings in some cases. Adv Phys Chem 2012:17. doi:10.1155/2012/720197
7. McKee ML (1993) Theoretical study of the interaction of gallium atoms with methane, ethylene, 1,3-butadiene, and benzene. J Am Chem Soc 115(21):9608–9613. doi:10.1021/ja00074a028
8. Knight JLB, Banisaukas Iii JJ, Babb R, Davidson ER (1996) Electron spin resonance matrix isolation and ab initio theoretical investigations of $^{69,71}GaH_2$, $^{69,71}GaD_2$, $H^{69,71}GaCH_3$, and $D^{69,71}GaCD_3$. J Chem Phys 105(16):6607–6615. doi:10.1063/1.471974
9. Himmel H-J, Downs AJ, Greene TM, Andrews L (2000) Matrix photochemistry of gallium and indium atoms (M) in the presence of methane: formation and characterization of the divalent species CH_3MH and univalent species CH_3M. Organometallics 19(6):1060–1070. doi:10.1021/om990905p
10. Pacheco-Sanchez JH, Luna-Garcia H, Castillo S (2004) Ab initio study of the reactions of Ga(^{2}P, ^{2}S, and ^{2}P) with methane. J Chem Phys 120(9):4240–4246. doi:10.1063/1.1643892
11. Cimiraglia R, Persico M (1987) Recent advances in multireference second order perturbation CI: the CIPSI method revisited. J Comput Chem 8(1):39–47. doi:10.1002/jcc.540080105
12. Rubio J, Novoa JJ, Illas F (1986) Convergence of a multireference second-order mbpt method (CIPSI) using a zero-order wavefunction derived from an MS SCF calculation. Chem Phys Lett 126(1):98–102. doi:10.1016/0009-2614(86)85123-5
13. Pacheco-Sanchez JH, Castillo S, Luna-Garcia H, Novaro O (2007) Transition probabilities on Ga(^{2}P, ^{2}S, and ^{2}P)+CH_4 reactions. J Chem Phys 126(10):106103-1–106103-3. doi:10.1063/1.2711192
14. Burkholder TR, Andrews L (1993) Matrix infrared spectra of aluminum, gallium, and indium complexes with acetylene. Inorg Chem 32(11):2491–2496. doi:10.1021/ic00063a048
15. Jones PM, Kasai PH (1988) Gallium-ethylene complex: matrix isolation ESR study. J Phys Chem 92(5):1060–1061. doi:10.1021/j100316a014
16. Schmidt MW, Baldridge KK, Boatz JA, Elbert ST, Gordon MS, Jensen JH, Koseki S, Matsunaga N, Nguyen KA, Su S, Windus TL, Dupuis M, Montgomery JA (1993) General atomic and molecular electronic structure system. J Comput Chem 14(11):1347–1363. doi:10.1002/jcc.540141112
17. Lee C, Yang W, Parr RG (1988) Development of the Colle-Salvetti correlation-energy formula into a functional of the electron density. Phys Rev B 37(2):785–789. doi:10.1103/PhysRevB.37.785
18. Miehlich B, Savin A, Stoll H, Preuss H (1989) Results obtained with the correlation energy density functionals of becke and Lee, Yang and Parr. Chem Phys Lett 157(3):200–206. doi:10.1016/0009-2614(89)87234-3
19. Becke AD (1993) A new mixing of Hartree–Fock and local density-functional theories. J Chem Phys 98(2):1372–1377. doi:10.1063/1.464304
20. Hertwig RH, Koch W (1997) On the parameterization of the local correlation functional. What is Becke-3-LYP? Chem Phys Lett 268(5–6):345–351. doi:10.1016/s0009-2614(97)00207-8
21. Dunning TH (1989) Gaussian basis sets for use in correlated molecular calculations. I. The atoms boron through neon and hydrogen. J Chem Phys 90(2):1007–1023. doi:10.1063/1.456153
22. Wilson AK, Woon DE, Peterson KA, Dunning TH (1999) Gaussian basis sets for use in correlated molecular calculations. IX. The atoms gallium through krypton. J Chem Phys 110(16):7667–7676. doi:10.1063/1.478678
23. Császár P, Pulay P (1984) Geometry optimization by direct inversion in the iterative subspace. J Mol Struct 114:31–34. doi:10.1016/s0022-2860(84)87198-7
24. Frisch MJ et al. (2007) Gaussian 03, Revision D.02. Gaussian, Inc, Wallingford
25. Zhurko G. ChemCraft, version 1.6 (build 348). http://www.chemcraftprog.com. Accessed 20 Mar 2012
26. Dennington R, Keith T, Millam J (2009) GaussView 03. Semichem, Inc, Shawnee Mission
27. Gonzalez C, Schlegel HB (1989) An improved algorithm for reaction path following. J Chem Phys 90(4):2154–2161. doi:10.1063/1.456010

28. Gonzalez C, Schlegel HB (1990) Reaction path following in mass-weighted internal coordinates. J Phys Chem 94(14):5523–5527. doi:10.1021/j100377a021
29. Pople JA, Head-Gordon M, Fox DJ, Raghavachari K, Curtiss LA (1989) Gaussian-1 theory: a general procedure for prediction of molecular energies. J Chem Phys 90(10):5622–5629. doi:10.1063/1.456415
30. Curtiss LA, Redfern PC, Raghavachari K (2005) Assessment of Gaussian-3 and density-functional theories on the G3/05 test set of experimental energies. J Chem Phys 123(12):124107–124112. doi:10.1063/1.2039080
31. Ikenaga M, Nakamura K, Tachibana A, Matsumoto K (2002) Quantum chemical study of gas-phase reactions of trimethylaluminium and triethylaluminium with ammonia in III–V nitride semiconductor crystal growth. J Cryst Growth 237–239(Part 2 (0)):936–941. doi:10.1016/s0022-0248(01)02002-4
32. Creighton JR, Wang GT (2005) Kinetics of metal organic−ammonia adduct decomposition: implications for group-III nitride MOCVD. J Phys Chem A 109(46):10554–10562. doi:10.1021/jp054380s
33. Moscatelli D, Cavallotti C (2007) Theoretical investigation of the gas-phase kinetics active during the GaN MOVPE. J Phys Chem A 111(21):4620–4631. doi:10.1021/jp068318m
34. Timoshkin AY, Bettinger HF, Schaefer HF (2001) DFT modeling of chemical vapor deposition of GaN from organogallium precursors. 1. Thermodynamics of elimination reactions. J Phys Chem A 105(13):3240–3248. doi:10.1021/jp002379h
35. Timoshkin AY, Bettinger HF, Schaefer HF (2001) DFT modeling of chemical vapor deposition of GaN from organogallium precursors. 2. Structures of the oligomers and thermodynamics of the association processes†. J Phys Chem A 105(13):3249–3258. doi:10.1021/jp002380g
36. Grimme S, Ehrlich S, Goerigk L (2011) Effect of the damping function in dispersion corrected density functional theory. J Comput Chem 32(7):1456–1465. doi:10.1002/jcc.21759
37. Grimme S, Antony J, Ehrlich S, Krieg H (2010) A consistent and accurate ab initio parametrization of density functional dispersion correction (DFT-D) for the 94 elements H-Pu. J Chem Phys 132(15). doi:10.1063/1.3382344
38. Hujo W, Grimme S (2012) Performance of dispersion-corrected density functional theory for thermochemistry and non-covalent interactions. J Cheminformatics 4(Suppl 1):P56. doi:10.1186/1758-2946-4-S1-P56
39. Gadzhiev OB, Ignatov SK, Razuvaev AG, Masunov AE (2009) Quantum chemical study of trimolecular reaction mechanism between nitric oxide and oxygen in the gas phase. J Phys Chem A 113(32):9092–9101. doi:10.1021/jp900484s
40. Gadzhiev OB, Ignatov SK, Gangopadhyay S, Masunov AE, Petrov AI (2011) Mechanism of nitric oxide oxidation reaction ($2NO+O_2 \rightarrow 2NO_2$) revisited. J Chem Theory Comput 7(7):2021–2024. doi:10.1021/ct100754m
41. Cheron N, Jacquemin D, Fleurat-Lessard P (2012) A qualitative failure of B3LYP for textbook organic reactions. Phys Chem Chem Phys 14(19):7170–7175. doi:10.1039/C2CP40438A
42. Grüber R, Fleurat-Lessard P (2014) Performance of recent density functionals to discriminate between olefin and nitrogen binding to palladium. Theor Chem Accounts 133(9):1–10. doi:10.1007/s00214-014-1533-2
43. West AC, Kretchmer JS, Sellner B, Park K, Hase WL, Lischka H, Windus TL (2009) $O(^3P)+C_2H_4$ potential energy surface: study at the multireference level†. J Phys Chem A 113(45):12663–12674. doi:10.1021/jp905070z
44. Gadzhiev OB, Ignatov SK, Krisyuk BE, Maiorov AV, Gangopadhyay S, Masunov AE (2012) Quantum chemical study of the initial step of ozone addition to the double bond of ethylene. J Phys Chem A 116(42):10420–10434. doi:10.1021/jp307738p
45. Krisyuk BE, Maiorov AV, Mamin EA, Popov AA (2013) Calculation of the effect of double bond strain in 1-chloroethylene and 1,1-dichloroethylene on the rate and mechanism of their reactions with ozone. Kinet Catal 54(2):149–156. doi:10.1134/s0023158413020092
46. Krisyuk BE, Maiorov AV, Mamin EA, Popov AA (2013) Quantum chemical study of the addition of ozone to acetylene. Kinet Catal 54(3):290–296. doi:10.1134/s0023158413030099
47. Kurtén T, Donahue NM (2012) MRCISD studies of the dissociation of vinylhydroperoxide, CH_2CHOOH: there is a saddle point. J Phys Chem A 116(25):6823–6830. doi:10.1021/jp302511a
48. Corchado JC, Coitiño EL, Chuang Y-Y, Fast PL, Truhlar DG (1998) Interpolated variational transition-state theory by mapping. J Phys Chem A 102(14):2424–2438. doi:10.1021/jp9801267
49. Chuang Y-Y, Corchado JC, Truhlar DG (1999) Mapped interpolation scheme for single-point energy corrections in reaction rate calculations and a critical evaluation of dual-level reaction path dynamics methods. J Phys Chem A 103(8):1140–1149. doi:10.1021/jp9842493
50. Neese F (2012) The ORCA program system. Wiley Interdiscip Rev Comput Mol Sci 2(1):73–78. doi:10.1002/wcms.81
51. Neese F (2012) ORCA—an ab initio, DFT and semiempirical SCF-MO package, Version 2.9.0; Max-Planck-Institute for Bioinorganic Chemistry: Stiftstr. 34–36, 45470 Mülheim a.d. Ruhr, Germany
52. Maxwell GR (2004) Synthetic nitrogen products: a practical guide to the products and processes. Springer, London
53. Valtazanos P, Ruedenberg K (1986) Bifurcations and transition states. Theor Chem Accounts 69(4):281–307. doi:10.1007/bf00527705
54. Ess DH, Wheeler SE, Iafe RG, Xu L, Çelebi-Ölçüm N, Houk KN (2008) Bifurcations on potential energy surfaces of organic reactions. Angew Chem Int Ed 47(40):7592–7601. doi:10.1002/anie.200800918
55. Basilevsky MV, Shamov AG (1981) The local definition of the Optimum ascent path on a multi-dimensional potential energy surface and its practical application for the location of saddle points. Chem Phys 60(3):347–358. doi:10.1016/0301-0104(81)80170-x
56. Basilevsky MV (1982) The topography of potential energy surfaces. Chem Phys 67(3):337–346. doi:10.1016/0301-0104(82)85194-x
57. Basilevsky MV (1983) Modern development of the reaction coordinate concept. J Mol Struct THEOCHEM 103:139–152. doi:10.1016/0166-1280(83)85015-5
58. Basilevsky MV (1988) Topography of potential energy surfaces. Pure Appl Chem 55(2):207–212. doi:10.1351/pac198855020207
59. Quapp W, Hirsch M, Heidrich D (2004) An approach to reaction path branching using valley–ridge inflection points of potential-energy surfaces. Theor Chem Accounts 112(1):40–51. doi:10.1007/s00214-003-0558-8
60. Quapp W (1989) Gradient extremals and valley floor bifurcations on potential energy surfaces. Theor Chem Accounts 75(6):447–460. doi:10.1007/bf00527676
61. Bofill JM, Quapp W, Caballero M (2013) Locating transition states on potential energy surfaces by the gentlest ascent dynamics. Chem Phys Lett 583:203–208. doi:10.1016/j.cplett.2013.07.074
62. Bofill JM, Quapp W, Caballero M (2012) The variational structure of gradient extremals. J Chem Theory Comput 8(3):927–935. doi:10.1021/ct200805d
63. Quapp W (2008) Chemical reaction paths and calculus of variations. Theor Chem Accounts 121(5–6):227–237. doi:10.1007/s00214-008-0468-x
64. Quapp W (2004) How does a reaction path branching take place? A classification of bifurcation events. J Mol Struct 695–696:95–101. doi:10.1016/j.molstruc.2003.10.034
65. Minyaev RM, Quapp W, Schmidt B, Getmanskii IV, Koval VV (2013) Unusual reaction paths of SN2 nucleophile substitution reactions $CH_4+H^- \rightarrow CH_4+H^-$ and $CH_4+F^- \rightarrow CH_3F+H^-$: quantum chemical calculations. Chem Phys 425:170–176. doi:10.1016/j.chemphys.2013.08.014

66. Quapp W, Schmidt B (2011) An empirical, variational method of approach to unsymmetric valley-ridge inflection points. Theor Chem Accounts 128(1):47–61. doi:10.1007/s00214-010-0749-z
67. Quapp W, Bofill J, Aguilar-Mogas A (2011) Exploration of cyclopropyl radical ring opening to allyl radical by Newton trajectories: importance of valley-ridge inflection points to understand the topography. Theor Chem Accounts 129(6):803–821. doi:10.1007/s00214-011-0938-4
68. Sandhiya L, Kolandaivel P, Senthilkumar K (2013) Depletion of atmospheric ozone by nitrogen dioxide: a bifurcated reaction pathway. Theor Chem Accounts 132(9):1–13. doi:10.1007/s00214-013-1382-4
69. Yamamoto Y, Hasegawa H, Yamataka H (2011) Dynamic path bifurcation in the beckmann reaction: support from kinetic analyses. J Org Chem 76(11):4652–4660. doi:10.1021/jo200728t
70. Carpenter BK (2013) Energy disposition in reactive intermediates. Chem Rev 113(9):7265–7286. doi:10.1021/cr300511u
71. Fikri M, Bozkurt M, Somnitz H, Schulz C (2011) High temperature shock-tube study of the reaction of gallium with ammonia. Phys Chem Chem Phys 13(9):4149–4154. doi:10.1039/C0CP01373K
72. Xie Y, Yates BF, Schaefer HF (1990) The wealth of energetically low-lying isomers for very simple organometallic systems. The aluminum-acetylene (AlC_2H_2) system. J Am Chem Soc 112(2):517–523. doi:10.1021/ja00158a007
73. Lee TJ, Taylor PR (1989) A diagnostic for determining the quality of single-reference electron correlation methods. Int J Quantum Chem 36(S23):199–207. doi:10.1002/qua.560360824
74. Lee TJ (2003) Comparison of the T_1 and D_1 diagnostics for electronic structure theory: a new definition for the open-shell D_1 diagnostic. Chem Phys Lett 372(3–4):362–367. doi:10.1016/S0009-2614(03)00435-4
75. Oliveira B, Araújo RMU (2012) Theoretical aspects of binary and ternary complexes of aziridine···ammonia ruled by hydrogen bond strength. J Mol Model 18(6):2845–2854. doi:10.1007/s00894-011-1300-4
76. Lind MC, Garrison SL, Becnel JM (2010) Trimolecular reactions of uranium hexafluoride with water. J Phys Chem A 114(13):4641–4646. doi:10.1021/jp909368g
77. Beckers H, Zeng X, Willner H (2010) Intermediates involved in the oxidation of nitrogen monoxide: photochemistry of the cis-$N_2O_2{\cdot}O_2$ complex and of sym-N_2O_4 in solid Ne matrices. Chem Eur J 16(5):1506–1520. doi:10.1002/chem.200902406